SPATIOTEMPORAL EVOLUTION AND LAG EFFECT OF DROUGHT AND VEGETATION DYNAMICS IN SOUTHWEST CHINA

YANG, C. P. – WANG, Y. Q. – WU, J. J. – SHEN, H. Z. – MA, X. Y.*

Key Laboratory of Agricultural Soil and Water Engineering in Arid Area of Ministry of Education, Northwest A&F University, Yangling 712100, China
(e-mail: yang_cuiping@nwafu.edu.cn)

**Corresponding author*
e-mail: xma@nwafu.edu.cn

(Received 10th Feb 2022; accepted 20th May 2022)

Abstract. In this study, the temporal and spatial characteristics of drought and vegetation dynamics as well as the lag time of vegetation's response to drought in Southwest China were determined. The normalized difference vegetation index (NDVI) and standardized precipitation and evapotranspiration index (SPEI) were used to evaluate the effects of drought on vegetation and determine the response of vegetation to hydrological and climatic changes in different seasons and time scales. The results indicated that from 1970 to 2020, the climate in Southwest China showed a aridity trend with a decreasing rate of 0.024/10a. In autumn, the drought trend intensified, and 90.62% of the study area exhibited a trend toward drought; the most significant drought trend was in Yunnan Province ($P < 0.05$). On a seasonal level, the NDVI had a downward trend in summer, with a decrease rate of 0.033/10a and an increasing trend in spring, autumn, and winter, with increase rates of 0.016/10a, 0.009/10a, and 0.15/10a, respectively. The areas with the most obvious improvement in vegetation cover were southern Guangxi Province and eastern Sichuan Province, which had the fastest improvement rate, 0.24/10a. The NDVI was most sensitive to the 6-month SPEI (SPEI_6). The lag time of the NDVI for SPEI at different time scales was 1 month, whereas the lag time for SPEI_6 was up to 2 years. The time delay effect of the NDVI on drought in northwest Sichuan, west Yunnan, southeast Guizhou, and north Guangxi was significantly correlated ($P < 0.05$). The region with the weakest correlation between the NDVI and SPEI was the agricultural area in eastern Sichuan ($P > 0.05$). This study provides a crucial theoretical basis for water balance, ecosystem protection, and efficient water resource management in Southwest China.
Keywords: *drought, vegetation, lag effect, multi-time scale, Southwest China*

Introduction

A drought is usually a natural phenomenon in which the available water is significantly below normal levels for a given period of time and the water supply does not meet current needs (Vicente-Serrano et al., 2015). In the context of global climate change, which is mainly characterized by warming, drought has become a change trend that cannot be ignored, and the frequency and intensity of extreme droughts are increasing, as well as their destructiveness (Sahoo et al., 2015; Vicente-Serrano et al., 2012). For example, a drought in Southwest China in 2010 led to a great negative impact on the ecosystem and agricultural economy of the southwest (Li et al., 2019). Drought affects the vegetation growth status of ecosystems. Studying the sensitivity of vegetation to drought at different time scales and its response characteristics is crucial to understand the response mechanism of dynamic vegetation changes (Piao et al., 2011a, b).

Vegetation is the most sensitive component to climate change (Jiang et al., 2017; Qi et al., 2019). Using the SPEI to scale drought conditions and quantifying

http://www.aloki.hu ● ISSN 1589 1623 (Print) ● ISSN 1785 0037 (Online)
DOI: http://dx.doi.org/10.15666/aeer/2004_34473466

vegetation growth based on the NDVI and radial growth of vegetation, Vicente-Serrano et al. (2015) studied the response of vegetation to drought on a global scale. In vegetation studies, a large number of studies have shown that vegetation growth is susceptible to drought, and studies have found varying degrees of positive correlation between vegetation growth trends and SPEI in most regions (Zhang et al., 2019; Lawal et al., 2019). Liu et al. (2015) demonstrated that the annual maximum NDVI was positively correlated with the SPEI in Yunnan Province, China. Wang et al. (2016) found a strong and positive correlation between the NDVI and SPEI in arid and semiarid areas, China. Vegetation growth was not only affected by drought at the same time, but also by the cumulative and lagged effects of drought (Nils et al., 2018). The lagged effect of vegetation response to drought refers to the fact that vegetation growth conditions are affected not only by the current climatic conditions but also by the climate change in the previous period (Rippin et al., 2011; Hoover et al., 2018). Krishna et al. (2019) analyzed the effect of drought on vegetation based on SPEI index. They found that the effect of SPEI on monthly mean NDVI values at different time scales has a lag effect. Yao et al. (2020) found that meteorological drought has a lagged effect on crop growth at different seasonal scales. Zhao et al. (2020) pointed out that drought has an extensive cumulative effect on the growth of grassland on the Loess Plateau, and the drought and vegetation The time lag effect of drought affects 50% of the grasslands on the Loess Plateau. In addition, vegetation growth is also affected by a combination of many factors such as soil texture, hours of light, flooding, pests and diseases, grazing, and human activities (Wu et al., 2010; Liu et al., 2013).

A large number of studies have been done on vegetation growth conditions based on NDVI indices. And the research areas mainly include the interrelationship between spatial and temporal changes of vegetation and climate factors at regional scale, among which climate factors are mainly temperature and precipitation, and the single factor changes cannot give a comprehensive response to climate change (Li et al., 2015; Che et al., 2014; Sun et al., 2015; Wang et al., 2015). In this paper, the multi-temporal scale SPEI drought index can combine multiple climate factors to more accurately respond to the evolution of dryness and wetness in southwest China, and explore the response mechanism of vegetation to multi-temporal scale drought. However, research on the time-lag characteristics of vegetation growth and drought at different spatial scales in Southwest China remains limited. Therefore, this study investigated (1) the spatiotemporal evolution of drought at annual and seasonal scales based on an Mann–Kendall (MK) trend analysis, (2) the spatiotemporal characteristics of vegetation dynamics at annual and seasonal scales, and (3) the time-delay effect of the NDVI and SPEI at different time scales and spatial distribution patterns. We elucidated the response mechanism of vegetation dynamic changes to drought over multiple time scales and analyzed the time-lag effect of drought in Southwest China, providing a scientific basis for ecosystem protection and drought monitoring.

Materials and methods

Study area

The study area was in Southwest China (20°54’–34°19’N, 97°21’–112°04’E). The administrative region comprises Yunnan, Guizhou, Sichuan, Guangxi, and Chongqing (*Fig. 1a*). This area covers approximately 1.37×10^6 km^2, accounting for 14.34% of the

http://www.aloki.hu ● ISSN 1589 1623 (Print) ● ISSN 1785 0037 (Online)
DOI: http://dx.doi.org/10.15666/aeer/2004_34473466

country. The region is bounded by the Qinghai–Tibet Plateau in the west, and it is influenced by southwest and southeast monsoons in the south. The region's topography is complex; it features both plateaus and basins. Thus, it is a typical area with a variable climate. The climate type is mainly a subtropical monsoon climate. The average annual temperature in most areas is 14–24 °C, and the annual average precipitation is more than 900 mm; precipitation generally decreases from southeast to northwest, and the seasonal distribution of precipitation is extremely uneven (Zhu et al., 2017). Precipitation from May to October accounts for 80%–90% of that of the entire year. However, precipitation from November to April of the next year only accounts for 10%–20% of precipitation, and the annual precipitation variability in the entire region is generally between 10% and 20% (Zhao et al., 1997).

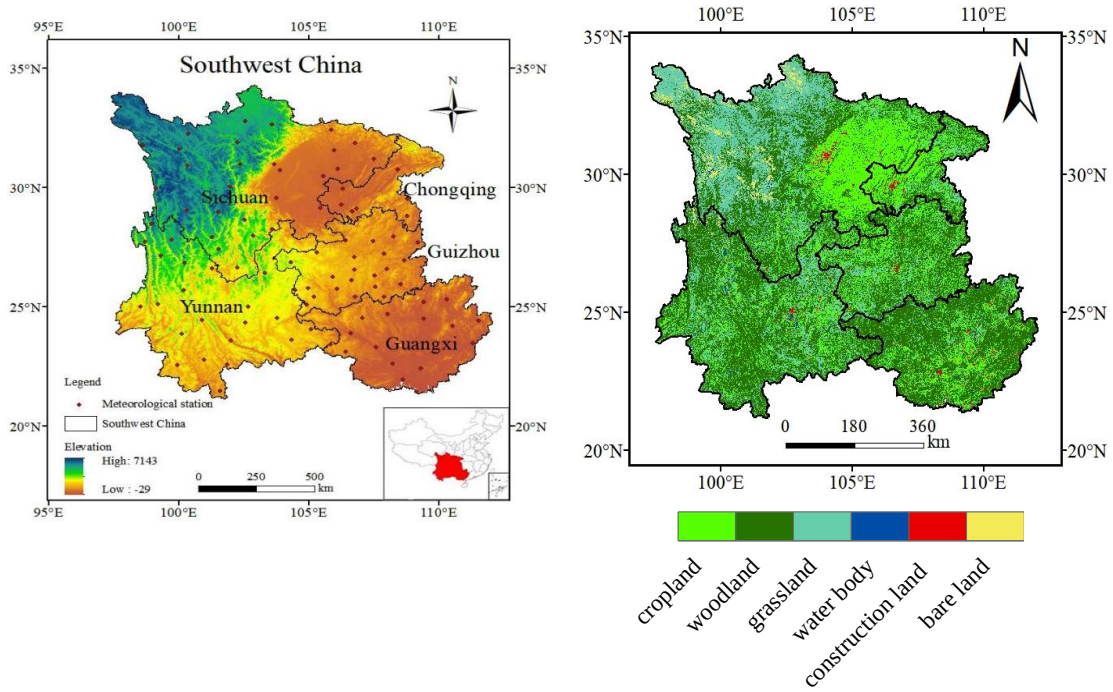

(a) (b)

Figure 1. *(a) Study area, comprising four provinces (Yunnan, Guizhou, Sichuan, and Guangxi) and a municipality (Chongqing) and (b) land use map in Southwest China*

Data sources and processing

In this study, daily average atmospheric pressure, average temperature, relative humidity, average wind speed, sunshine duration, and wind speed from 96 basic meteorological stations in Southwest China from 1970 to 2020 provided by China Meteorological Data Sharing Network (http://cdc.cma.gov.cn) were used, and the data with missing measurement values were interpolated using linear regression. Moderate-Resolution Imaging Spectroradiometer (MODIS) NDVI data were obtained from MODIS Terra satellite sensor data available in the MOD13Q1 data set (https://lpdaac.usgs.gov/products/mod13q1v006/); the year range for data is 2000 to 2020. The spatial resolution was 500 m × 500 m, and the temporal resolution was 16 d. In this study, the maximum value composite procedure was used to synthesize NDVI

http://www.aloki.hu ● ISSN 1589 1623 (Print) ● ISSN 1785 0037 (Online)
DOI: http://dx.doi.org/10.15666/aeer/2004_34473466

data into monthly values such that they corresponded to monthly SPEI values (Cong et al., 2012; Zhao et al., 2017). The SPEI data was resampled to match the MODIS NDVI data at 500 m spatial resolution by using a majority function in the Resample Tool of ArcGIS. Land use data are obtained from data Center for Resources and Environmental Sciences, Chinese Academy of Sciences. Scale 1:100,000; According to the national standard of Classification of Land Use Status (GB/T21010-2007), the land use in the study area was divided into six land use modes: cultivated land, forest land, grassland, water area, construction land and bare land.

Methods

Standardized precipitation and evapotranspiration index (SPEI)

The SPEI reflects the water balance between precipitation and evapotranspiration. It was devised by Vicente-Serrano et al. (2010), who introduced the concept of potential evapotranspiration based on the SPI. Beguería et al. (2014) improved the SPEI and used the Food and Agriculture Organization of the United Nations (FAO) Penman–Monteith (PM) equation to calculate evapotranspiration instead of using Thornthwaite's value. The PM equation has a clearer physical meaning and higher accuracy compared with Thornthwaite's value. The calculation formula is as follows:

(1) The PM equation was used to calculate potential evapotranspiration (ET_0)

$$ET_0 = \frac{0.408\Delta(R_n - G) + \gamma \frac{900}{T + 273} u_2 (e_s - e_a)}{\Delta + \gamma(1 + 0.34u_2)} \quad \text{(Eq.1)}$$

where ET_0 is the potential evapotranspiration (mm d^{-1}); $\Delta$is the slope of temperature changes with saturated vapor pressure (kPa °C^{-1}); R_n is the net radiation [MJ (m^2 d^{-1})]; and G is soil heat flux density [MJ (m^2 d^{-1})], which is small relative to R_n, especially when vegetation cover and calculation step size are equal to or close to 1 d; this value is ignored as 0. The hygrometer constant is represented by γ (kPa °C^{-1}); T is the average daily temperature (°C); u_2 is the wind speed at a height of 2 m (m s^{-1}), which can be converted from wind speed at 10 m; e_s is the saturated vapor pressure (kPa); and e_a is the actual vapor pressure (kPa).

(2) The difference between monthly precipitation and potential evapotranspiration is calculated as follows:

$$D_m = P_m - ET_0 \quad \text{(Eq.2)}$$

where m is the number of months, P_m is monthly precipitation, and ET_0 is the potential evapotranspiration.

(3) Pairs are clustered and normalized for different time scales as follows:

$$\begin{cases} D_{m,n}^{i} = \sum_{j=13-i+n}^{12} D_{m-1,j} + \sum_{j=1}^{n} D_{m,j}, n < i \\ D_{m,n}^{i} = \sum_{j=n-i+1}^{n} D_{m,j}, n \geq i \end{cases} \quad \text{(Eq.3)}$$

http://www.aloki.hu ● ISSN 1589 1623 (Print) ● ISSN 1785 0037 (Online)
DOI: http://dx.doi.org/10.15666/aeer/2004_34473466

where $D_{m,n}^{i}$ is the cumulative value of differences between precipitation and evapotranspiration in month *i* starting from the *n*th month of *m* year.

(4) The log-logistic probability distribution function was used to fit the D_m sequence and obtain the cumulative probability density function as follows:

$$F(D) = \left[1 + \left(\frac{\alpha}{D-\gamma}\right)^{\beta}\right]^{-1} \quad \text{(Eq.4)}$$

where parameters α, β, and γ represent the size, shape, and position parameters, respectively, estimated using the linear moment method.

The cumulative probability density is normalized using the following equations:

$$SPEI = W - \frac{c_1 + c_2 W + c_3 W^2}{1 + t_1 W + t_2 W^2 + t_3 W^3} \quad \text{(Eq.5)}$$

$$W = \sqrt{-2\ln(P)} \quad \text{(Eq.6)}$$

where P is the probability of a value being greater than a certain D_m value, $P \leq 0.5$, $P = 1 - F(D)$; $P = 1 - P$; $c_0 = 2.515517$, $c_1 = 0.802853$, $c_2 = 0.010328$, $t_1 = 1.432788$, $t_2 = 0.189269$, and $t_3 = 0.001308$.

The SPEI reveals degrees of dryness and wetness. The higher the SPEI value, the wetter an area, and the smaller the SPEI value, the drier an area. *Table 1* presents the corresponding classification of drought grades.

Table 1. *Standardized precipitation and evapotranspiration index (SPEI) drought classification*

Level	Type	SPEI
1	None	(-0.5,0.5)
2	Light drought	(-1,-0.5]
3	Moderate drought	(-1.5,-1]
4	Severe drought	(-2,-1.5]
5	Extreme drought	(-∞,-2]

Normalized difference vegetation index (NDVI)

The NDVI is a crucial remote-sensing parameter that provides information on plant growth and nutrition. The calculation formula is as follows:

$$NDVI = \frac{NIR - RED}{NIR + RED} \quad \text{(Eq.7)}$$

where *NIR* is near-infrared reflectance and *RED* is visible light reflectance. Areas with vegetation NDVI > 0.1 are usually considered to have vegetation cover, and an increase in NDVI indicates an increase in green vegetation; areas with NDVI < 0.1 indicate no

http://www.aloki.hu ● ISSN 1589 1623 (Print) ● ISSN 1785 0037 (Online)
DOI: http://dx.doi.org/10.15666/aeer/2004_34473466

vegetation cover, such as construction land, bare soil, desert, Gobi, water bodies, snow and ice, and clouds.

Trend analysis method

(1) Mann-Kendall (MK) trend test

The MK trend test is nonparametric, and it can distinguish whether the sequence variability trend is deterministic or stochastic without following a specific distribution and is widely used in meteorological and hydrological studies (Mann et al., 1945; Kendall et al., 1975).

With n time series exist of sample size ($x_1,\ldots,x_n$), for all k, $j \le n$ and $k \ne j$ and different distributions for x_k and x_j, test statistic S can be calculated as follows:

$$S = \sum_{i=1}^{n-1} \sum_{j=i+1}^{n} \mathrm{sgn}(x_j - x_i) \tag{Eq.8}$$

$$\mathrm{sgn}(x_j - x_i) = \begin{cases} 1, x_j - x_i > 0 \\ 0, x_j - x_i = 0 \\ -1, x_j - x_i < 0 \end{cases} \tag{Eq.9}$$

$$Var(S) = \frac{n(n-1)(2n+5) - \sum_{i-1}^{m} t_i(t_i-1)(2t_i+5)}{18} \tag{Eq.10}$$

When $n > 10$, the standard normal statistical variable can be derived as follows:

$$Z = \begin{cases} \dfrac{S-1}{\sqrt{Var(S)}}, S > 0 \\ 0, S = 0 \\ \dfrac{S+1}{\sqrt{Var(S)}}, S < 0 \end{cases} \tag{Eq.11}$$

If the Z value is regular, an upward trend is exhibited; if the Z value is negative, a downward trend is exhibited.

Trends were detected at specific significance levels (α). When $|Z| > Z_{1-\alpha/2}$, the null hypothesis that a significant trend would exist in the time series was rejected. $Z_{1-\alpha/2}$ was obtained from the standard normal distribution table. Significance levels (α) of 0.01 and 0.05 were used in this study. At the 5% significance level, for $|Z| > 1.96$, the null hypothesis was rejected. At the 1% significance level, for $|Z| > 2.576$, the null hypothesis was rejected.

(2) Linear regression analysis

The least square method was applied to the slope (gradient) of the trend line to dynamically analyze vegetation changes in Southwest China. The calculation formula is as follows:

http://www.aloki.hu ● ISSN 1589 1623 (Print) ● ISSN 1785 0037 (Online)
DOI: http://dx.doi.org/10.15666/aeer/2004_34473466

$$\lambda_{slope} = \frac{n\sum_{i=1}^{n} i \times C_i - \sum_{i=2}^{n} i \sum_{i=1}^{n} C}{n\sum_{i=1}^{n} i^2 - \left(\sum_{i=1}^{n} i\right)^2} \quad \text{(Eq.12)}$$

where λ_{slope} is the slope of the trend line, n is the study time, and Ci is the NDVI of year i.

Correlation analysis

Correlation coefficient R between the NDVI and SPEI at different time scales is calculated as follows:

$$R = \frac{\sum_{i=1}^{n}(x_i - \bar{x})(y_i - \bar{y})}{\sqrt{\sum_{i=1}^{n}(x_i - \bar{x})^2 \sum_{i=1}^{n}(y_i - \bar{y})^2}} \quad \text{(Eq.13)}$$

where x_i and y_i represent SPEI and NDVI values in the ith year, respectively, and x and y are the average SPEI and NDVI values over the study years, respectively.

Results and analysis

Temporal and spatial variations in drought characteristics in Southwest China

Figure 2 illustrates the annual and seasonal variations in the SPEI for Southwest China. The 3-month SPEI value (SPEI_3) was selected to analyze the characteristics for seasonal SPEI variations, and the 12-month SPEI (SPEI_12) was used analyze the characteristics for annual SPEI variations. *Figure 2* reveals that the SPEI for Southwest China had a downward trend during 1970–2020, an upward trend during 1970–2000 with a slope of 0.0107, and a sharp decline after 2000. A large-scale severe drought event occurred in Southwest China in 2010 (Cheng et al., 2019) (*Fig. 2*). However, at a seasonal level, the autumn SPEI in Southwest China exhibited a downward trend from 1970 to 2000 with a slope of −0.0171, indicating that the autumn drought was exacerbated, whereas the autumn SPEI indicated wetter conditions from 2001 to 2020. From 1970 to 2020, the SPEI of Southwest China has exhibited a trend of drought.

The Z statistic of the MK trend analysis of 96 meteorological stations was calculated to analyze variations in SPEI at annual and seasonal levels in Southwest China (*Fig. 3*). Annually, SPEI values exhibited a downward trend ($Z < 0$) in 55.21% of Southwest China, mainly concentrated in Yunnan Province, Chongqing City, and southeast Sichuan Province. The SPEI in 8.33% of the area exhibited a significant downward trend ($Z \leq -1.96$, $P < 0.05$), mainly distributed in Yunnan Province, which indicates a significant trend of drought in Yunnan Province from 1970 to 2020. The regions with increased SPEI ($Z > 0$) values were mainly distributed in northern Sichuan, Guizhou, and Guangxi. The SPEI increased significantly ($Z \geq 1.96$, $P < 0.05$) in the northwest of Sichuan Province, indicating that the climate in this region was humid. At the seasonal

http://www.aloki.hu ● ISSN 1589 1623 (Print) ● ISSN 1785 0037 (Online)
DOI: http://dx.doi.org/10.15666/aeer/2004_34473466

level, he SPEI increased significantly in 7.29% of the study area ($Z \geq 1.96$, $P < 0.05$) in spring; this increase was mainly in southern Yunnan Province, eastern Sichuan Province, and northern Guangxi Province. In summer, the SPEI values in Sichuan, Guizhou, and Guangxi Provinces exhibited an increasing trend, whereas in Yunnan Province, the SPEI values indicated a trend toward drought. In autumn, the SPEI of 90.62% of the study area exhibited a downward trend ($Z < 0$) of drought, and 11.46% of the area had a significant downward trend of drought ($Z \leq -1.96$, $P < 0.05$). The main distribution areas were the east and south of Yunnan Province, which indicated that the autumn drought trend in Southwest China has increased in the past 51 years, with the autumn drought in Yunnan Province having the most significant upward trend.

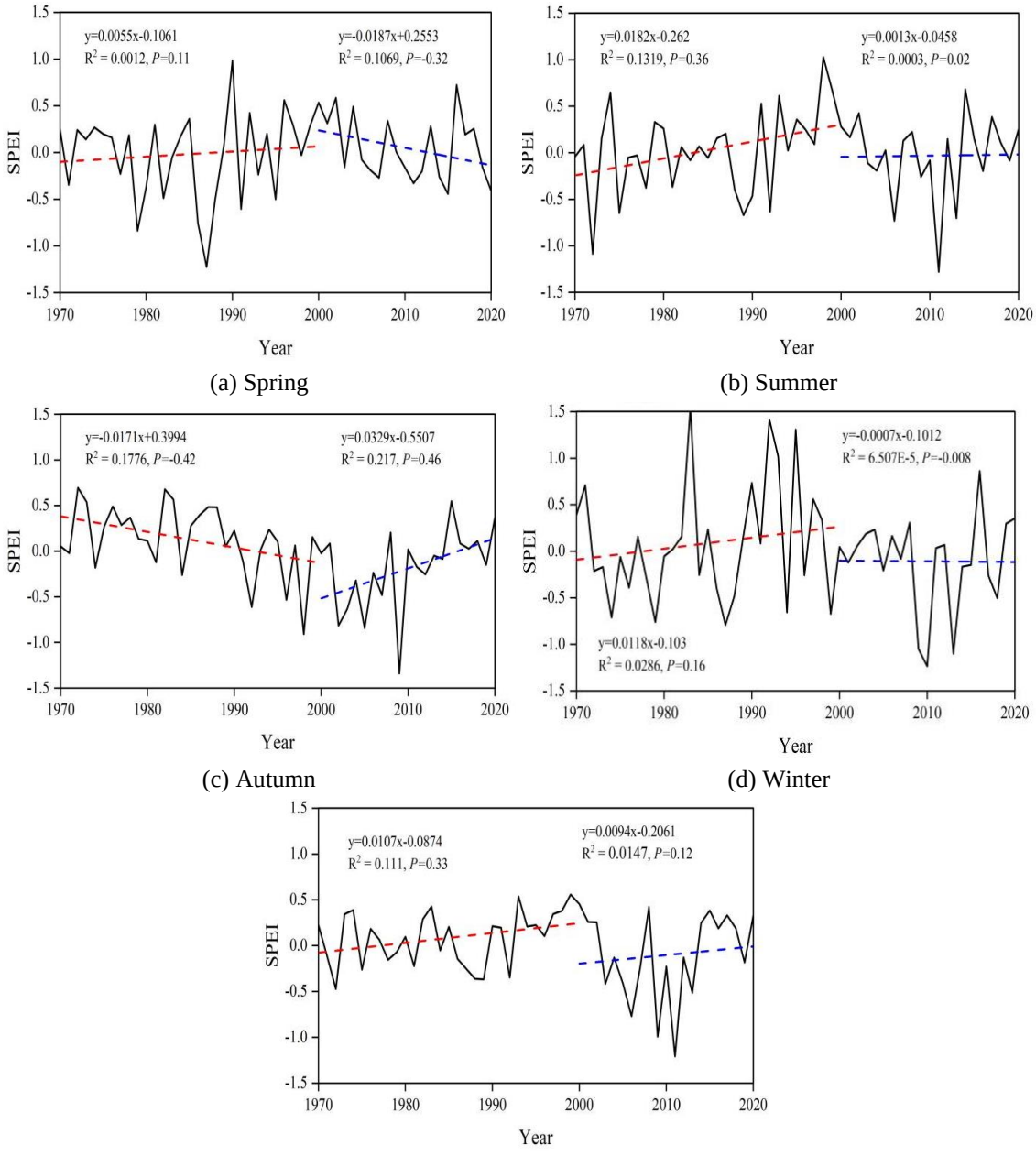

Figure 2. *Annual and seasonal variations in the SPEI in Southwest China from 1970 to 2020*

http://www.aloki.hu ● ISSN 1589 1623 (Print) ● ISSN 1785 0037 (Online)
DOI: http://dx.doi.org/10.15666/aeer/2004_34473466

In winter, the SPEI in 52.08% of the study area exhibited a downward trend ($Z < 0$), and in 9.38% of the area, it had a significant downward trend ($Z \leq -1.96$, $P < 0.05$), which was mainly distributed in eastern Sichuan (the Sichuan Basin). Generally, most of Southwest China had a trend of drought during 1970–2020. This trend was most pronounced in autumn. The spatial distributions of drought in Southwest China were diverse, while the trend of aridification was most serious in Yunnan Province.

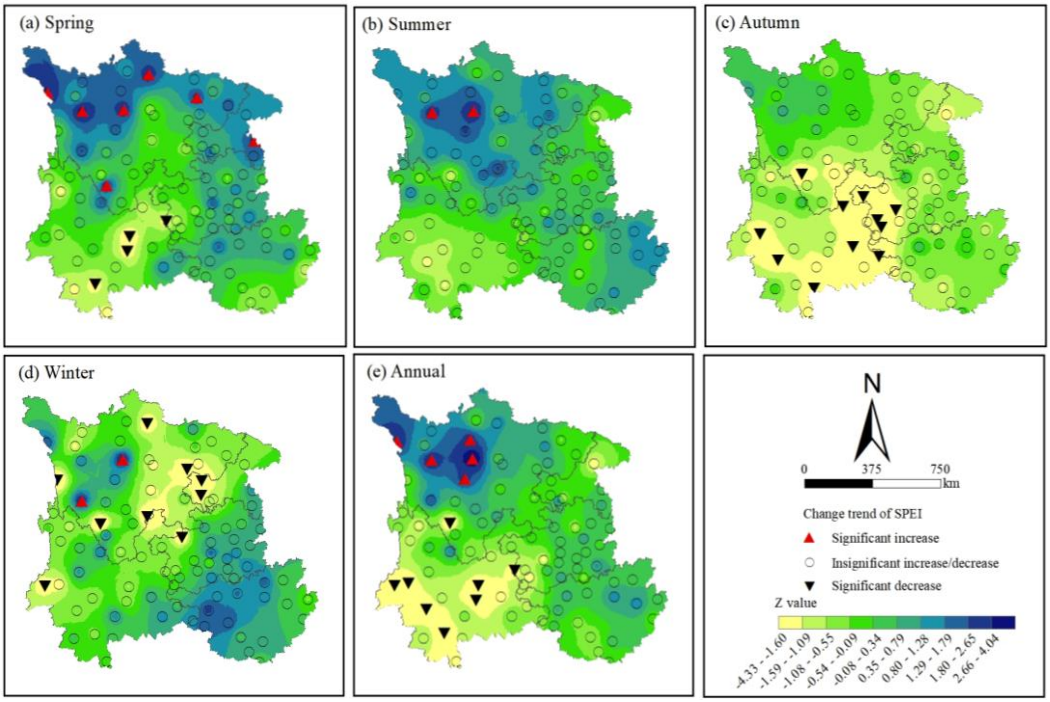

Figure 3. *Spatial distribution and variations in the SPEI yearly from 1970 to 2020 in Southwest China as well as in spring, summer, autumn, and winter*

Dynamic spatiotemporal changes in vegetation cover in Southwest China

The results of a linear trend analysis (*Fig. 4*) revealed that the annual average NDVI in Southwest China decreased slightly from 2000 to 2020, but the change was relatively stable. In summer, the NDVI decreased at a rate of 0.033/10a, whereas in spring, autumn, and winter, the NDVI increased slowly at a rate of 0.016/10a, 0.009/10a, and 0.015/10a, respectively.

Figure 5 displays the significant spatial heterogeneity of NDVI trends in Southwest China. *Figure 5a* presents the spatial distribution of annual mean NDVI in Southwest China, and *Figure 5b* depicts the regional changes in average NDVI slope from 2000 to 2020. Because of the complex topographic and geomorphological conditions in Southwest China, the annual average NDVI exhibited an obvious upward trend, ranging from −0.09 to 0.82. The NDVI value in the southwest region of the study area is larger, whereas that in the northwest is smaller. This is because the northwest region is located on the Zoige Plateau, and the high altitude affects climate conditions, resulting in sparse vegetation coverage, such as forest and grassland. Therefore, the NDVI is generally below 0.43, whereas in most other areas, it is above 0.43. In terms of NDVI trend variations, 55.21% of the study area

http://www.aloki.hu ● ISSN 1589 1623 (Print) ● ISSN 1785 0037 (Online)
DOI: http://dx.doi.org/10.15666/aeer/2004_34473466

exhibited a decreasing trend during 2000–2020, with 29.16% of the area exhibiting a significant decreasing trend ($P < 0.05$). The average annual NDVI exhibited an increasing trend in the remaining 44.79% of the area, of which 28.12% had a significant increasing trend ($P < 0.05$). In summary, the NDVI trend distribution in Southwest China indicated a zonal change from east to west; the trend decreased at first, increased, and then decreased.

The areas with the most obvious improvement in vegetation cover were southern Guangxi Province and eastern Sichuan Province, which had the fastest improvement rate of 0.24/10a (*Fig. 5b*). However, the NDVI in southern Guangxi Province, northeastern Guizhou Province, northeastern Sichuan Province, and some areas of Yunnan Province exhibited negative trends; these areas had a trend of vegetation degradation, and the fastest degradation rate was 0.36/10a, which is higher than the maximum vegetation improvement rate (0.24/10a). This trend was observed because vegetation coverage was affected by high altitude and human activities.

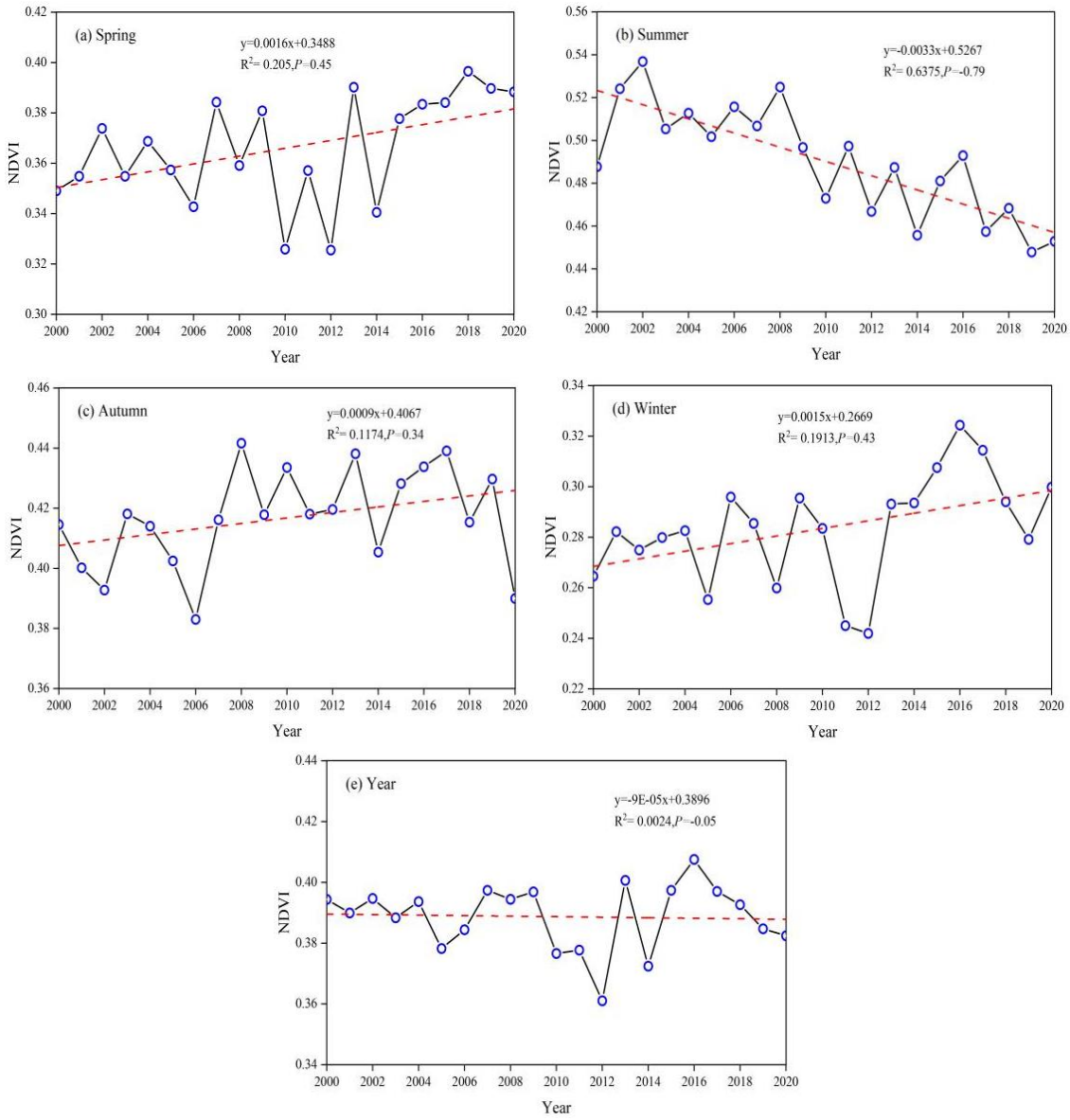

Figure 4. *Annual and seasonal NDVI trends in Southwest China from 2000 to 2020*

http://www.aloki.hu ● ISSN 1589 1623 (Print) ● ISSN 1785 0037 (Online)
DOI: http://dx.doi.org/10.15666/aeer/2004_34473466

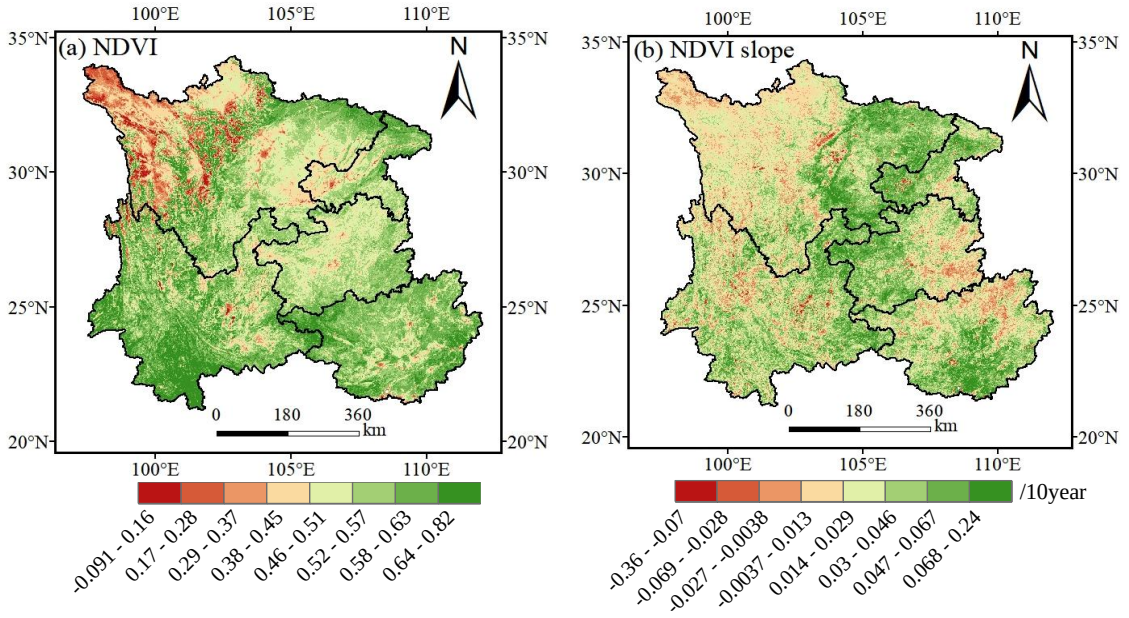

Figure 5. *(a) Annual average normalized difference vegetation index (NDVI) values and (b) slopes of annual normalized difference vegetation index (NDVI) variation in Southwest China from 2000 to 2020*

Analysis of the lag effect between the NDVI and SPEI at different time scales in Southwest China

The spatial distribution of correlation coefficients between the NDVI and SPEI at different time scales in Southwest China were analyzed. With consideration of the lag effect of the NDVI on drought, the lag correlation between the NDVI and SPEI was further analyzed. The correlation between the NDVI (NDVI for the year, 1-month lagged NDVI series, 3-month lagged NDVI series, 6-month lagged NDVI series, 1-year lagged NDVI series, and 2-year lagged NDVI series) and 1-month SPEI (SPEI_1), 3-months SPEI (SPEI_3), 6-month SPEI (SPEI_6), and 12-months SPEI (SPEI_12) was investigated. The proportions of areas for which the correlation coefficient between the NDVI and SPEI passed the significance test ($P < 0.05$) are also presented (*Fig. 6; Tables 2* and 3).

The results indicated that over time, the correlation between the NDVI and SPEI increased, and the correlation between the NDVI and SPEI_6 was the most significant. The correlation between 1 month lagged NDVI and SPEI_6 was the highest ($R = 0.227$, $P < 0.01$), followed by the correlation between 2-year lagged NDVI and SPEI_6 ($R = 0.171$, $P < 0.01$; *Table 2*). The regions with significant correlations ($P < 0.05$) between the NDVI at different lag times (NDVI for the year, 1-month lagged NDVI series, 3-month lagged NDVI series, 6-month lagged NDVI series, 1-year lagged NDVI series, and 2-year lagged NDVI series) and the SPEI_6 accounted for 22.92%, 35.42%, 17.71%, 13.54%, 20.83% and 15.63% (*Table 3*) in Southwest China, respectively. Therefore, responses of the NDVI to the SPEI at different time scales in Southwest China had a lag effect of 1 month, and the lag effect of the NDVI and SPEI_6 could reach up to 2 years. The correlations of different time scales indicated that droughts are among the most important factors affecting vegetation growth in the study area. The results verified the hypothesis that vegetation growth has a delayed response to drought.

http://www.aloki.hu ● ISSN 1589 1623 (Print) ● ISSN 1785 0037 (Online)
DOI: http://dx.doi.org/10.15666/aeer/2004_34473466

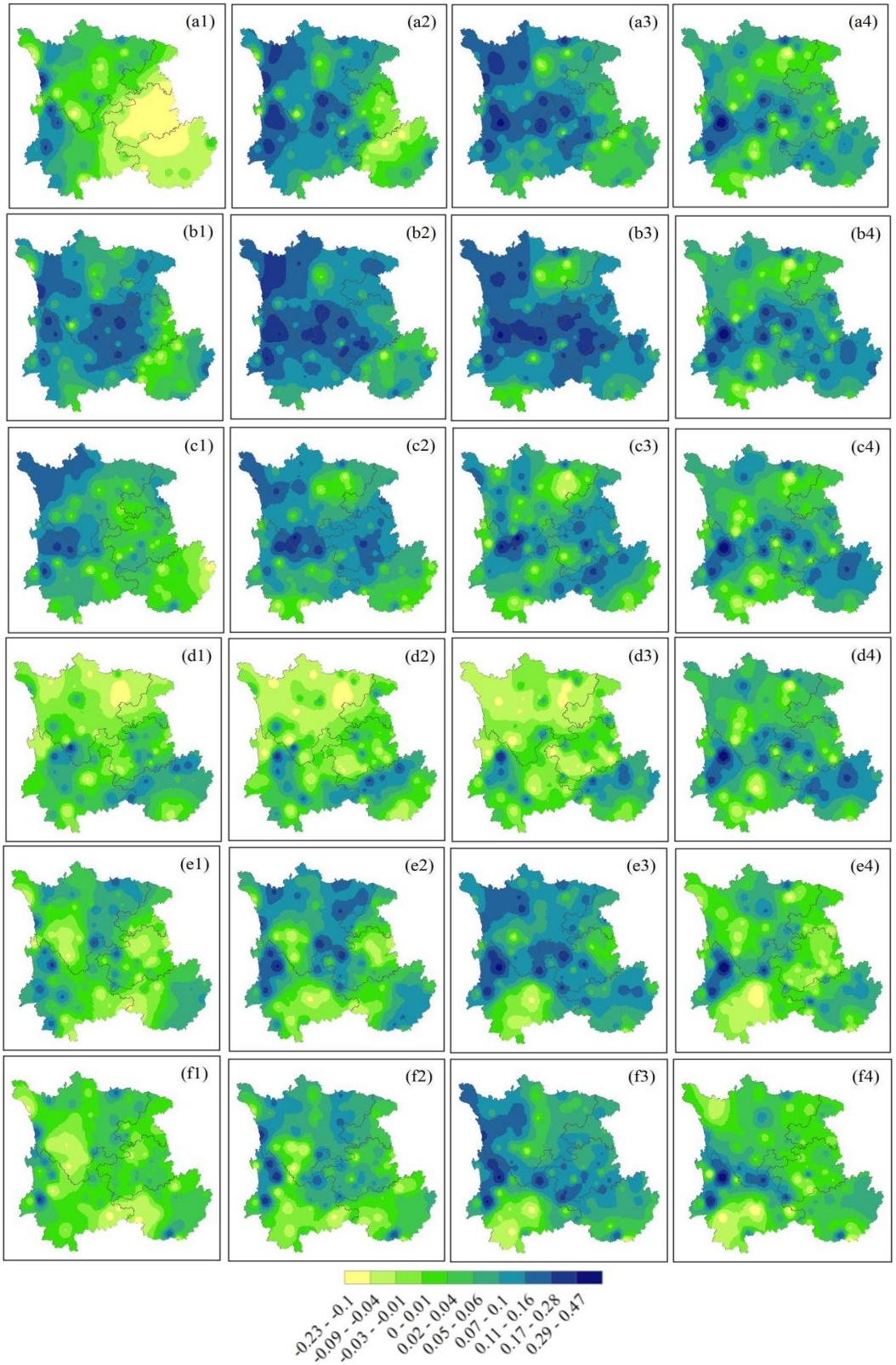

Figure 6. *Spatial distribution of correlation coefficients between annual mean NDVI and SPEI at different time scales in Southwest China (a, b, c, d, e, and f denote NDVI for the year, 1-month lagged NDVI series, 3-month lagged NDVI series, 6-month lagged NDVI series, 1-year lagged NDVI series, and 2-year lagged NDVI series, respectively; 1, 2, 3, 4 denote 1-month, 3-month, 6-month, and 12-month SPEI, respectively)*

http://www.aloki.hu ● ISSN 1589 1623 (Print) ● ISSN 1785 0037 (Online)
DOI: http://dx.doi.org/10.15666/aeer/2004_34473466

According to the spatial distribution patterns related to the correlation coefficient, the regions with significant correlations between the NDVI and SPEI ($P < 0.05$) in Southwest China were mainly distributed in northwest Sichuan (the Zoige Plateau), west Yunnan (the Hengduan Mountains), southeast Guizhou (the Yunnan–Guizhou Plateau), and northern Guangxi. In east Sichuan (the Sichuan Basin), the correlation between the NDVI and SPEI was small compared with that in other regions, indicating that the regional vegetation changes induced by drought were small. This was because this region is mainly agricultural (*Fig. 1b*); crop growth requires irrigation, and thus, the correlation between vegetation and climate change was weak.

Table 2. *Correlation coefficients between annual mean NDVI and SPEI at different time scales in Southwest China from 2000 to 2020*

NDVI	SPEI_1	SPEI_3	SPEI_6	SPEI_12
NDVI for the year	-0.059	0.107	0.162	0.053
1-month lagged NDVI series	0.128*****	0.203******	0.227******	0.085
3-months lagged NDVI series	0.094	0.185******	0.132******	0.094
6-months lagged NDVI series	0.026	-0.031	-0.069	0.078
1-year lagged NDVI series	0.004	0.105	0.169******	0.007
2-year lagged NDVI series	0.022	0.116	0.171******	0.037

*****Statistically significant at the 5% level. ******Statistically significant at the 1% level

Table 3. *Proportion of areas in which the correlation coefficient between the NDVI and SPEI was significant*

	Area ratio (%)			
	SPEI_1	SPEI_3	SPEI_6	SPEI_12
NDVI for the year	22.92	16.67	22.92	10.42
1-month lagged NDVI series	22.92	29.17	35.42	19.79
3-months lagged NDVI series	11.46	16.67	17.71	14.58
6-months lagged NDVI series	7.29	12.50	13.54	15.63
1-year lagged NDVI series	5.21	15.63	20.83	9.38
2-year lagged NDVI series	5.21	9.38	15.63	10.42

Discussion

Vegetation growth is influenced by climatic factors such as precipitation and temperature. Koutsodendris et al. (2018) found that with increasing temperatures, the return of vegetation to green at high latitudes in the Northern Hemisphere was advanced. The effect of precipitation on vegetation growth varies in different regions, where NDVI is significantly and positively correlated with precipitation in arid and semi-arid regions as well as in monsoon climate zones. Especially, the most important constraint for the germination and growth period of vegetation in arid zones is precipitation (Jha et al., 2018). Vegetation growth in harsh environments, such as those with drought, generates corresponding drought resistance through self-regulatory mechanisms. Studies have demonstrated that different vegetation types have different drought resistance, with the lag effect of extreme drought on forest vegetation being up to 4 years, while the response period for grassland is only 1 year (Dash et al., 2019; Xu

http://www.aloki.hu ● ISSN 1589 1623 (Print) ● ISSN 1785 0037 (Online)
DOI: http://dx.doi.org/10.15666/aeer/2004_34473466

et al., 2018), which is explained by the soil water is distributed in different proportions at different soil depths in different types of vegetation areas (Wu et al., 2018; Girardin et al., 2016). With increasing soil thickness, the soil water content in forested areas gradually increases, thus resisting drought at longer time scales. Therefore, the response of vegetation to drought displays a lag effect.

Li et al. (2020) analyzed the lag effect of the NDVI on precipitation in each climatic region of China, and they found that the lag time differed significantly among different climatic zones. The vegetation growth in the arid regions of northwest China is governed by precipitation, which can promote the early growth of vegetation in the growing season and therefore has a relatively short lag time. However, in southwest China, where precipitation is abundant and vegetation is mainly forested, the lag time in response to drought is relatively long. This study revealed that by contrast with changes in the summer and annual SPEI, the NDVI exhibited a decreasing trend, and the minimum annual NDVI (0.36) was in 2012 (*Fig. 4e*), whereas the corresponding minimum SPEI (−1.21) appeared in 2011 (*Fig. 2e*), confirming the lag effect between the NDVI and climate change. In a study on Southwest China, the correlation between NDVI and drought indices, with a lag of approximately 1 month, was high, and the lag time was significant (Li et al., 2019). Our study concluded that the response of vegetation in Southwest China to drought at different times lagged by 1 month, whereas the lag effect of SPEI_6, which is the most sensitive to drought response by NDVI, can reach up to 2 years' time, and the above studies are basically consistent with the conclusion of this study.

The response of the NDVI to drought varies with topographic features, elevation, vegetation type, and human activities (Ghebrezgabher et al., 2020; Guan et al., 2020). In terms of spatial distribution, the correlations between the NDVI and SPEI were high and significant in northwest Sichuan Province (the Ruoerge Plateau), west Yunnan Province (the Hengduan Mountains), southeast Guizhou Province (the Yunnan–Guizhou Plateau), and northern Guangxi Province, whereas the correlations between the NDVI and SPEI were weak and mostly nonsignificant in eastern Sichuan Province (the Sichuan Basin). These findings were related to the complex geomorphological conditions of the study area. Northwest Sichuan Province, west Yunnan Province, and southeast Guizhou Province are high-altitude areas, and precipitation and temperature conditions in the region are the most influential factors governing vegetation dynamics; thus, the NDVI and SPEI in this region have a strong correlation. In the eastern part of Sichuan, where crop growth is dominant, anthropogenic disturbances such as irrigation and fertilization create favorable conditions for crop growth, and thus, the correlation between the NDVI and SPEI in this region is low (Li et al., 2018). The NDVI and SPEI exhibited a mainly weak positive correlation and a partially negative correlation; the main reason for these results is that vegetation growth is less influenced by moisture, and temperature becomes the main factor affecting vegetation growth due to terrain conditions (Thavorntam et al., 2013).

This study mainly explored the influence of climatic factors on vegetation dynamics in Southwest China. Subsequent studies should explore other factors that may affect vegetation growth, such as topographic and geomorphological features, soil physical and chemical properties, and human economic activities (Gouveia et al., 2017; Lai et al., 2018). Some studies have confirmed that the NDVI is generally increasing in Southwest China, but marshes and grasslands have exhibited a decreasing trend. Zhou et al. (2018) found a significant increase in annual mean NDVI in high-altitude

http://www.aloki.hu ● ISSN 1589 1623 (Print) ● ISSN 1785 0037 (Online)
DOI: http://dx.doi.org/10.15666/aeer/2004_34473466

subalpine scrub in southwest China. Liu et al. (2015) found that vegetation growth was closely related to groundwater level, and the groundwater level in the best vegetation growth area in the Qaidam River basin was 1.70 m, for example. In economically and socially developed areas such as the Yangtze River Delta, a trend of NDVI reduction is exhibited at all time scales, which indicating that urbanization development has adversely affected vegetation cover, and that the physical characteristics of vegetation are influenced by factors such as the expansion of traffic roads, high population density, and the heat island effect (Xu et al., 2017; Rmg et al., 2019). Therefore, multiple influencing factors should be integrated to analyze vegetation dynamic changes in subsequent studies.

Conclusions

The dynamic evolution of drought and vegetation cover in Southwest China was analyzed using the SPEI and NDVI to identify the seasons and regions with the most severe aridification trends and to reveal the time lag effect of vegetation dynamics on drought. The main conclusions are as follows:

(1) The whole area of Southwest China presented a trend of aridity. The most significant trend of drought was in autumn, with 90.62% of the regions exhibiting a decrease in SPEI. The regions exhibiting a significant decrease in SPEI were mainly in Yunnan Province, and those with a significant increase were mainly in northwestern Sichuan.

(2) In spatially, the NDVI changes in strips from east to west, with the most obvious the greatest vegetation growth in southern Guangxi Province and eastern Sichuan Province.

(3) The NDVI response to different SPEI time scales in Southwest China had a 1-month lag effect, and the longest lag effect for the NDVI was for SPEI_6 (up to 2 years).

This research had crucial implications for drought monitoring and vegetation conservation in Southwest China. However, the response of vegetation evolution to various influencing factors, such as land use, soil texture, and human activities would be further explored.

Acknowledgements. This study was financially supported by The National Natural Science Foundation of China, grant number 51279167; Distributed Monitoring and Forecasting Technology of Soil Moisture in Irrigation District (No.2017YFC0403202).

REFERENCES

[1] Beguería, S., Vicente-Serrano, S. M., Reig, F., Latorre, B. (2014): Standardized precipitation evapotranspiration index (SPEI) revisited: parameter fitting, evapotranspiration models, tools, datasets and drought monitoring. – International Journal of Climatology 34(10): 3001-3023.

[2] Che, M., Chen, B., Innes, J. L. et al. (2014): Spatial and temporal variations in the end date of the vegetation growing season throughout the Qinghai-Tibetan Plateau from 1982 to 2011. – Agricultural and Forest Meteorology 189: 81-90.

[3] Cheng, Q., Gao, L., Zuo, X., Zhong, F. (2019): Statistical analyses of spatial and temporal variabilities in total, daytime, and nighttime precipitation indices and of extreme

http://www.aloki.hu ● ISSN 1589 1623 (Print) ● ISSN 1785 0037 (Online)
DOI: http://dx.doi.org/10.15666/aeer/2004_34473466

dry/wet association with large-scale circulations of Southwest China, 1961-2016. – Atmospheric Research 219: 166-182.
[4] Cong, N., Piao, S., Chen, A., Wang, X., Lin, X., Chen, S., Han, S., Zhou, G., Zhang, X. (2012): Spring vegetation green-up date in China inferred from SPOT NDVI data: a multiple model analysis. – Agric For Meteorol 165: 104-113.
[5] Dash, S., Sahoo, B., Raghuwanshi, N. (2019): A SWAT-Copula based approach for monitoring and assessment of drought propagation in an irrigation command. – Ecological Engineering 127: 417-430.
[6] Ghebrezgabher, M., Yang, T., Yang, X. (2020): Assessment of NDVI variations in responses to climate change in the Horn of Africa. – Egyptian Journal of Remote Sensing and Space Science 23(03): 249-261.
[7] Girardin, M., Hogg, E., Bernie, P. (2016): Negative impacts of high temperatures on growth of black spruce forests intensify with the anticipated climate warming. – Global Change Biology 22: 627-643.
[8] Gouveia, C., Trigo, R., Begueria, S., Vicente-Serrano, S. M. (2017): Drought impacts on vegetation activity in the Mediterranean region: an assessment using remote sensing data and multi-scale drought indicators. – Glob Planet Chang 151: 15-27.
[9] Guan, Y., Lu, H., Yin, C. (2020): Vegetation response to climate zone dynamics and its impacts on surface soil water content and albedo in China. – Science of the Total Environment 747: 141-153.
[10] Hoover, R., Gayloro, D., Cooper, C. (2018): Dune mobility in the St. Anthony Dune Field, Idaho, USA: effects of meteorological variables and lag time. – Geomorphology 309: 29-37.
[11] Jha, S., Srivastava, R. (2018): Impact of drought on vegetation carbon storage in arid and semi-arid regions. – Remote Sensing Applications: Society and Environment 11: 22-29.
[12] Jiang, L., Jiapaer, G., Bao, A., Guo, H., Ndayisaba, F. (2017): Vegetation dynamics and responses to climate change and human activities in Central Asia. – Science of the Total Environment 599: 967-980.
[13] Kendall, M. (1975): Rank Correlation Methods. – Griffin, London.
[14] Koutsodendris, A., Allstädt, F., Kern, O., Kousis, I. (2019): Late Pliocene vegetation turnover on the NE Tibetan Plateau (Central Asia) triggered by early Northern Hemisphere glaciation. – Elsevier 180: 117-125.
[15] Krishna, R., William, R. (2019): Satellite-based vegetation optical depth as an indicator of drought-driven tree mortality. – Remote Sensing of Environment 227: 471-482.
[16] Lai, C., Li, J., Wang, Z., Wu, X., Zeng, Z., Chen, X., Lian, Y., Yu, H., Wang, P., Bai, X. (2018): Drought induced reduction in net primary productivity across mainland China from 1982 to 2015. – Remote Sens 10: 1-27.
[17] Lawal, S., Lennard, C., Jack, C. (2019): The observed and model-simulated response of southern African vegetation to drought. – Agricultural and Forest Meteorology 279: 534-542.
[18] Li, S., Yang, S., Liu, X. (2015): NDVI based analysis on the influence of climate change and human activities on vegetation restoration in the Shaanxi-Gansu-Ningxia region, Central China. – Remote Sensing 7(9): 11163-11182.
[19] Li, K., Tong, Z., Liu, X. (2018): Quantitative assessment and driving force analysis of vegetation drought risk to climate change: methodology and application in Northeast China. – Agricultural and Forest Meteorology 8: 282-283.
[20] Li, X., Li, Y., Chen, A. (2019): The impact of the 2009/2010 drought on vegetation growth and terrestrial carbon balance in Southwest China. – Agricultural and Forest Meteorology 269: 239-248.
[21] Li, Q., Shi, X., Wu, Q. (2020): Exploring suitable topographical factor conditions for vegetation growth in Wanhuigou catchment on the Loess Plateau, China: a new perspective for ecological protection and restoration. – Ecological Engineering 158: 106-114.

http://www.aloki.hu ● ISSN 1589 1623 (Print) ● ISSN 1785 0037 (Online)
DOI: http://dx.doi.org/10.15666/aeer/2004_34473466

[22] Liu, Y., Lei, H. (2015): Responses of natural vegetation dynamics to climate drivers in China from 1982 to 2011. – Remote Sensing 7(8): 10243-10268.
[23] Liu, M., Qin, P., Liu, K. (2013): Response of lake water level of Honghu Lake to SPEI/SPI drought indices at different time scales. – Meteorological Monthly 39(9): 1163-1170.
[24] Liu, S., Tian, Y., Yin, Y., An, N., Dong, S. (2015): Effects of climate change on normalized difference vegetation index based on the multiple analysis of standardized precipitation evapotranspiration index methods in the Lancang River basin. – Climatic and Environmental Research 20: 705-714.
[25] Mann, H. (1945): Nonparametric tests against trend. – Econometrica 13: 245-259.
[26] Nils, H., Peter, S., Christian, A. (2018): Drought sensitivity and stem growth variation of nine alien and native tree species on a productive forest site in Germany. – Agricultural and Forest Meteorology 256/257: 431-444.
[27] Piao, S., Wang, X., Ciais, P., Zhu, B., Wang, T., Liu, J. (2011a): Changes in satellite-derived vegetation growth trend in temperate and boreal Eurasia from 1982 to 2006. – Glob. Change Biol 17: 3228-3239.
[28] Piao, S., Cui, M., Chen, A., Wang, X., Ciais, P., Liu, J., Tang, Y. (2011b): Altitude and temperature dependence of change in the spring vegetation green-up date from 1982 to 2006 in the Qinghai-Xizang Plateau. – Agricultural and Forest Meteorology 151: 1599-1608.
[29] Qi, X., Jia, J., Liu, H., Lin, Z. (2019): Relative importance of climate change and human activities for vegetation changes on China's silk road economic belt over multiple timescales. – Catena 180: 224-237.
[30] Rippin, D., Carrivick, J., Williams, C. (2011): Evidence towards a thermal lag in the response of Karsaglaciaren, northern Sweden, to climate change. – Journal of Glaciology 57(205): 895-903.
[31] Rmg, A., As, B., Haaq, A. (2019): A fuzzy model integrating shoreline changes, NDVI and settlement influences for coastal zone human impact classification. – Applied Geography 113: 267-277.
[32] Sahoo, A., Sheffield, J., Pan, M. (2015): Evaluation of the tropical rainfall measuring mission multi-satellite precipitation analysis (TMPA) for assessment of large-scale meteorological drought. – Remote Sens. Environ 159: 181-193.
[33] Shiru, M., Shahid, S., Chung, E. (2019): Changing characteristics of meteorological droughts in Nigeria during 1901-2010. – Atmospheric Research 223: 60-73.
[34] Sun, W., Song, X., Mu, X. (2015): Spatiotemporal vegetation cover variations associated with climate change and ecological restoration in the Loess Plateau. – Agricultural and Forest Meteorology 209: 87-99.
[35] Thavorntam, W., Tantemsapya, N. (2013): Vegetation greenness modeling in response to climate change for Northeast Thailand. – Journal of Geographical Sciences 23: 1052-1068.
[36] Vicente-Serrano, S. M., Beguería, S., Lorenzo-Lacruz, J. I. (2010): A multiscalar drought index sensitive to global warming: the standardized precipitation evapotranspiration index. – Journal of Climate 23(7): 1696-1718.
[37] Vicente-Serrano, S. M., Beguería, S., Lorenzo-Lacruz, J. I. (2012): Performance of drought indices for ecological, agricultural, and hydrological applications. – Earth Interact 16: 1-27.
[38] Vicente-Serrano, S. M., Gouveia, C., Camarero, J. (2013): Response of vegetation to drought time-scales across global land biomes. – Proceedings of the National Academy of Sciences 110(1): 52-57.
[39] Vicente-Serrano, S., Cabello, D., Tomásburguera, M. (2015): Drought variability and land degradation in semiarid regions: assessment using remote sensing data and drought indices (1982-2011). – Remote Sensing 7: 4391-4423.

http://www.aloki.hu ● ISSN 1589 1623 (Print) ● ISSN 1785 0037 (Online)
DOI: http://dx.doi.org/10.15666/aeer/2004_34473466

[40] Wang, H., Chen, Y., Pan, Y. (2015): Spatial and temporal variability of drought in the arid region of China and its relationships to teleconnection indices. – Journal of Hydrology 523: 283-296.
[41] Wang, Z., Huang, Z., Li, J. (2016): Assessing impacts of meteorological drought on vegetation at catchment scale in China based on SPEI and NDVI. – Transactions of the Chinese Society of Agricultural Engineering 32(14): 177-186.
[42] Wu, P., Zhao, X. (2010): Impact of climate change on agricultural water use and grain production in China. – Transactions of the Chinese Society of Agricultural Engineering 26(2): 1-6.
[43] Wu, X., Liu, H., Li, X. (2018): Differentiating drought legacy effects on vegetation growth over the temperate Northern Hemisphere. – Global Change Biology 24: 504-516.
[44] Xu, Y., Xu, Y., Wang, Y. (2017): Spatial and temporal trends of reference crop evapotranspiration and its influential variables in Yangtze River Delta, eastern China. – Theoretical and Applied Climatology 130(3/4): 945-958.
[45] Xu, H., Wang, X., Zhao, C. (2018): Diverse responses of vegetation growth to meteorological drought across climate zones and land biomes in northern China from 1981 to 2014. – Agricultural and Forest Meteorology 262: 1-13.
[46] Yao, N., Zhao, H., Li, Y., Biswas, A. (2020): National-scale variation and propagation characteristics of meteorological, agricultural, and hydrological droughts in China. – Remote Sensing 12(20): 256-264.
[47] Zhang, X., Zhang, B. (2019): The responses of natural vegetation dynamics to drought during the growing season across China. – Journal of Hydrology 574: 706-714.
[48] Zhao, J. (1997): Physical Geography of China. 4th Ed. – Higher Education Press, Beijing.
[49] Zhao, A., Yu, Q., Feng, L. (2020): Evaluating the cumulative and time-lag effects of drought on grassland vegetation: a case study in the Chinese Loess Plateau. – Journal of Environmental Management 261: 110214.
[50] Zhou, Q., Luo, Y., Zhou, X., Cai, M., Zhao, C. (2018): Response of vegetation to water balance conditions at different time scales across the karst area of southwestern China-A remote sensing approach. – Science of the Total Environment 645: 460-470.
[51] Zhu, G., Qin, D., Liu, Y., et al. (2017): Accuracy of TRMM precipitation data in the southwest monsoon region of China. – Theoretical and Applied Climatology 129(1/2): 353-362.

APPENDIX

Table A1. *The list of the 96 meteorological stations in Southwest China*

Station number	Province	Station name	Latitude (°)	Longitude (°)	Elevation (m)
56144	Sichuan	Dege	31.80	98.58	3201.2
56146	Sichuan	Ganzi	31.62	100.00	3393.5
56152	Sichuan	Seda	32.28	100.33	3893.9
56172	Sichuan	Maerkang	31.90	102.23	2669.8
56173	Sichuan	Hongyuan	32.80	102.55	3462.9
56178	Sichuan	Xiaojin	31.00	102.35	2367
56182	Sichuan	Songpan	32.65	103.57	2827.7
56187	Sichuan	Wenjiang	30.75	103.87	539.1
56188	Sichuan	Dujiangyan	31.00	103.67	706.7
56247	Sichuan	Batang	30.00	99.10	2589.2
56251	Sichuan	Xinlong	30.93	100.32	3000
56357	Sichuan	Daocheng	29.05	100.30	3727.7

http://www.aloki.hu ● ISSN 1589 1623 (Print) ● ISSN 1785 0037 (Online)
DOI: http://dx.doi.org/10.15666/aeer/2004_34473466

56374	Sichuan	Kangding	30.05	101.97	2615.7
56386	Sichuan	Leshan	29.57	103.75	424.2
56444	Yunnan	Deqin	28.48	98.92	3588.6
56459	Sichuan	Muli	27.93	101.27	2666.6
56462	Sichuan	Jiulong	29.00	101.50	2987.3
56475	Sichuan	Yuexi	28.65	102.52	1661.6
56479	Sichuan	Zhaojue	28.00	102.85	2132.4
56485	Sichuan	Leibo	28.27	103.58	1474.9
56533	Yunnan	Gongshan	27.75	98.67	1591.3
56543	Yunnan	Zhongdian	27.83	99.70	3276.1
56548	Yunnan	Weixi	27.17	99.28	2325.6
56565	Sichuan	Yanyuan	27.43	101.52	2439.4
56651	Yunnan	Lijiang	26.85	100.22	2393.2
56664	Yunnan	Huaping	26.63	101.27	1244.8
56671	Sichuan	Huili	26.65	102.25	1788.4
56684	Yunnan	Huize	26.42	103.28	2109.5
56691	Guizhou	Weining	26.87	104.28	2234.5
56739	Yunnan	Tengchong	25.02	98.50	1647.8
56748	Yunnan	Baoshan	25.12	99.18	1653.5
56751	Yunnan	Dali	25.70	100.18	1990.5
56778	Yunnan	Kunming	25.00	102.65	1891.4
56792	Guizhou	Puan	25.78	104.97	1620
56793	Guizhou	Panxian	25.72	104.47	1527.1
56856	Yunnan	Jingdong	24.47	100.87	1162.3
56875	Yunnan	Yuxi	24.33	102.55	1636.5
56886	Yunnan	Lixi	24.53	103.77	1704.3
56951	Yunnan	Lincang	23.88	100.08	1463.5
56954	Yunnan	Lancang	22.57	99.93	1054.8
56964	Yunnan	Simao	22.78	100.97	1302.1
56966	Yunnan	Yuanjiang	23.60	101.98	396.6
56969	Yunnan	Mengla	21.48	101.57	639.1
56977	Yunnan	Jiangcheng	22.58	101.85	1119.5
56991	Yunnan	Yanshan	23.62	104.33	1554
57206	Sichuan	Guangyuan	32.43	105.85	487
57306	Sichuan	Langzhong	31.58	105.97	382.2
57313	Sichuan	Bazhong	31.87	106.77	358.7
57328	Sichuan	Daxian	31.20	107.50	310.4
57405	Sichuan	Suining	30.50	105.55	278.2
57411	Sichuan	Nanchong	30.78	106.10	297.7
57432	Chongqing	Wanxian	30.77	108.40	186.7
57512	Chongqing	Hechuan	29.97	106.28	230.6
57517	Chongqing	Jiangjin	29.28	106.25	208.6
57536	Chongqing	Qianjiang	29.53	108.78	635.7
57606	Guizhou	Tongzi	29.13	106.83	972
57608	Sichuan	Xuyong	29.17	105.43	377.5
57612	Chongqing	Qijiang	29.02	106.65	252.7

http://www.aloki.hu ● ISSN 1589 1623 (Print) ● ISSN 1785 0037 (Online)
DOI: http://dx.doi.org/10.15666/aeer/2004_34473466

57633	Chongqing	Youyang	28.83	108.77	663.7
57707	Guizhou	Jijie	27.30	105.28	1510.6
57710	Guizhou	Renhuai	27.80	106.40	850
57718	Guizhou	Xifeng	27.10	106.73	1038.1
57722	Guizhou	Meitan	27.77	107.47	791.8
57729	Guizhou	Yuqing	27.23	107.88	600
57731	Guizhou	Sinan	27.95	108.25	416.3
57741	Guizhou	Tongren	27.72	109.18	283.5
57806	Guizhou	Anshun	26.25	105.90	1392.9
57816	Guizhou	Guiyang	26.58	106.73	1071.2
57825	Guizhou	Kaili	26.60	107.98	720.3
57827	Guizhou	Duyun	26.32	107.53	760
57832	Guizhou	Sansui	26.97	108.67	610.5
57902	Guizhou	Xingyi	25.43	105.18	1378.5
57907	Guizhou	Xingyi	25.08	104.90	1305
57910	Guizhou	Ziyun	25.77	106.08	1161
57912	Guizhou	Huishui	26.13	106.63	949.7
57916	Guizhou	Luodian	25.43	106.77	440.3
57922	Guizhou	Dushan	25.83	107.55	972.2
57926	Guizhou	Libo	25.42	107.88	432.9
57932	Guizhou	Rongjiang	25.97	108.53	325.1
57947	Guangxi	Rongan	25.22	109.40	119.7
57957	Guangxi	Guilin	25.32	110.30	166.7
59007	Yunnan	Guangnan	24.07	105.07	1250.5
59021	Guangxi	Fengshan	24.55	107.03	485.1
59023	Guangxi	Hechi	24.70	108.03	214.4
59046	Guangxi	Liuzhou	24.52	109.40	96.9
59058	Guangxi	Mengshan	24.20	110.52	144
59065	Guangxi	Hexian	24.42	111.53	108
59209	Guangxi	Napo	23.42	105.83	794.7
59211	Guangxi	Baise	23.90	106.60	173.1
59218	Guangxi	Jingxi	23.13	106.42	739.1
59228	Guangxi	Pingguo	23.32	107.58	107.8
59265	Guangxi	Wuzhou	23.48	111.30	119.2
59431	Guangxi	Nanning	22.63	108.22	72.2
59446	Guangxi	Lingshan	22.42	109.30	65.6
59632	Guangxi	Qinzhou	21.95	108.62	4
59644	Guangxi	Beihai	21.45	109.13	14.6

http://www.aloki.hu ● ISSN 1589 1623 (Print) ● ISSN 1785 0037 (Online)
DOI: http://dx.doi.org/10.15666/aeer/2004_34473466